Ion-induced nanopatterning of semiconductor surfaces

A short link between basic research and applications

Rossana Dell'Anna

MNF - FBK

It-fab Italian Network for Micro and Nano Fabrication

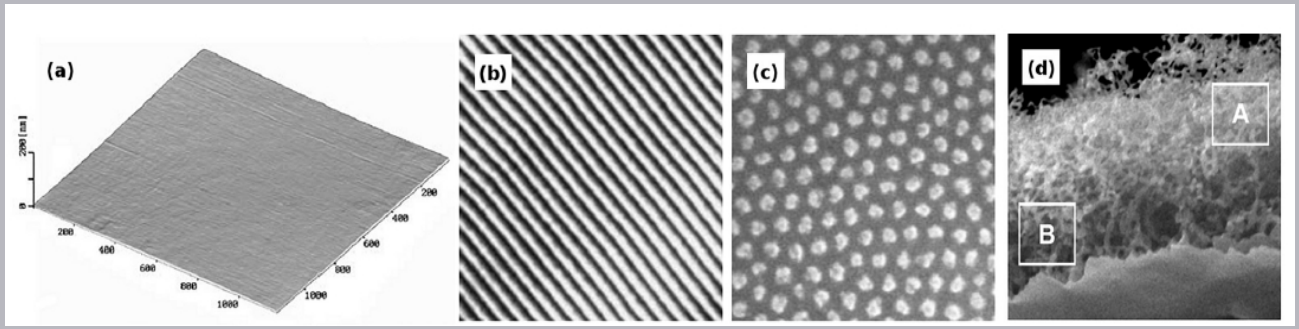

S. Norris et al., Appl. Phys. Rev.2019, 6, 011311

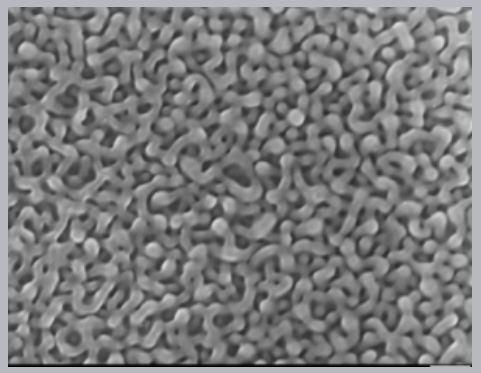

R. Dell'Anna et al, JPCM 30 (32), 324001

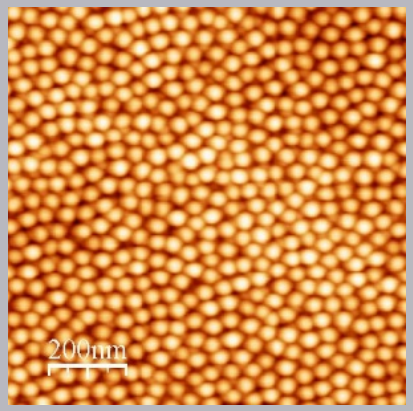

S. Facsko et al. APL, 2002, 80, 130

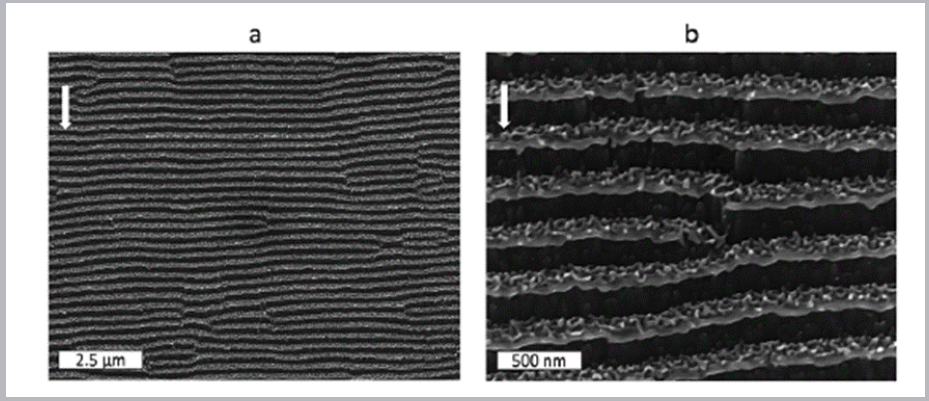

R. Dell'Anna, C. Masciullo et al., RSC Adv., 2017, 7, 9024

Taniguchi et al, 1974

Erosion of solid targets through ion beam irradiation as a promising technique to nanostructure the surface of a wide range of materials.

"Nanotechnology"

Experimental pattern control

Variation in the induced nanostructures by changing:

- Incident ion species
- Angle of ion incidence ϑ
- Energy of incident ions E
- Ion fluence Φ
- Substrate temperature T
- Target material

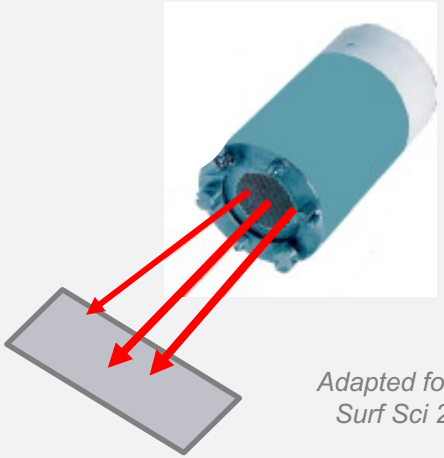

Adapted form Lloyd et al. Surf Sci 2016, 653, 334

nanopatterning by IBI in brief

Q. Wei et al., Adv. Mater 2009, 21 2865

Implicit characteristics:

- self-organizing phenomenon
- one step process
- short time
- large surface area (high output)
- sub-micrometer and nanometer length scales

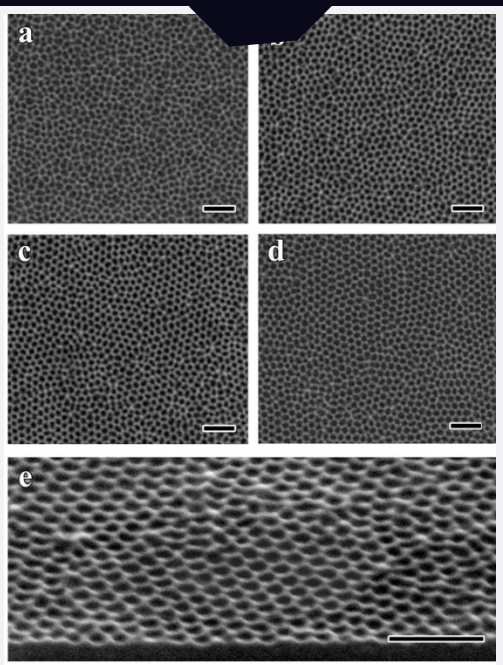

Complementary with respect to lithographic techniques

R. Dell'Anna et al, JPCM 30 (32), 324001

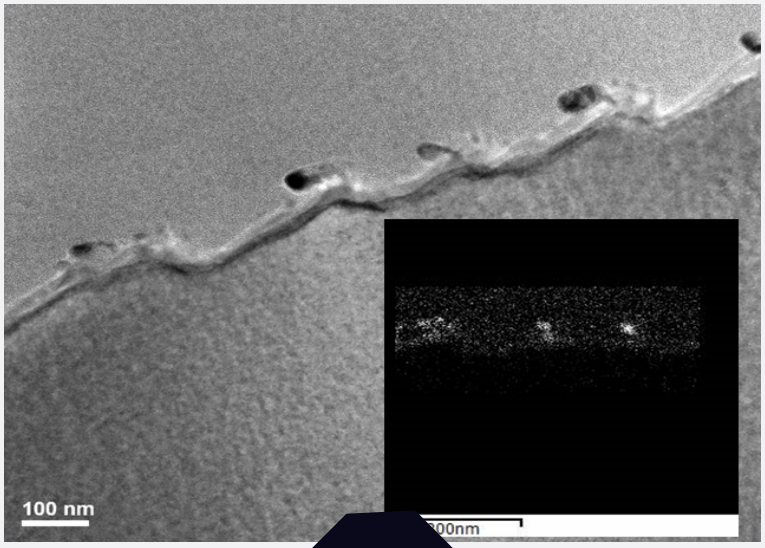

- Fabrication of different possible nanostructures
- on different materials (semiconductors, metals, insulators)

- Through the ion species, chemical engineering of the surface

Different possible application fields

pattern production in a controlled & reproducible fashion

thorough knowledge

physical main mechanisms driving the phenomenon

merging

of theory and experiments

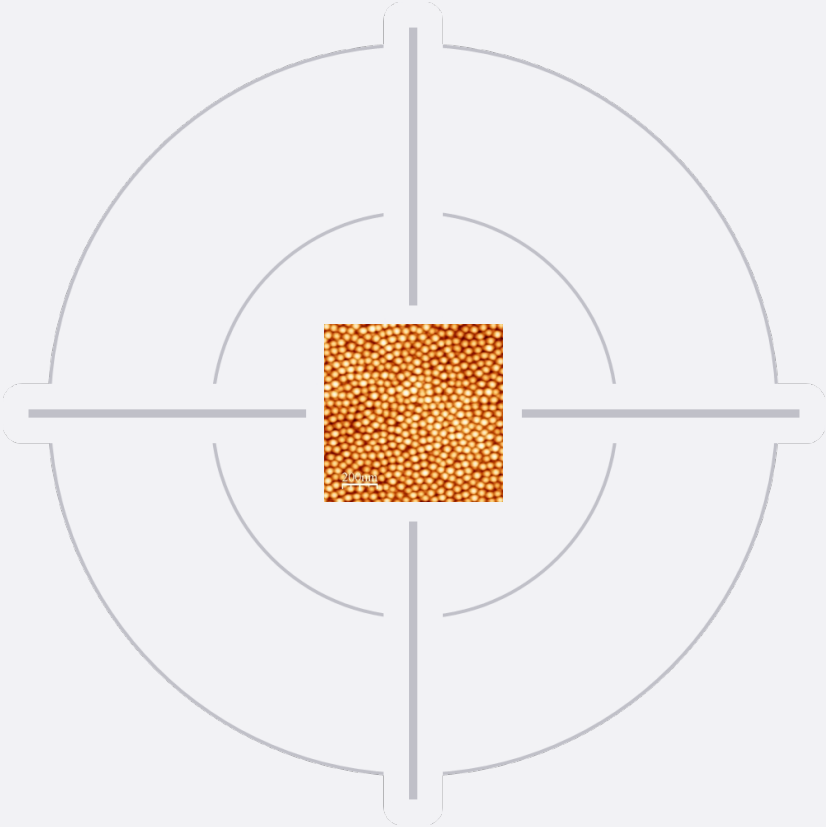

precise control

of size, shape, composition

Cascades of atomic displacements by energetic ion impacts

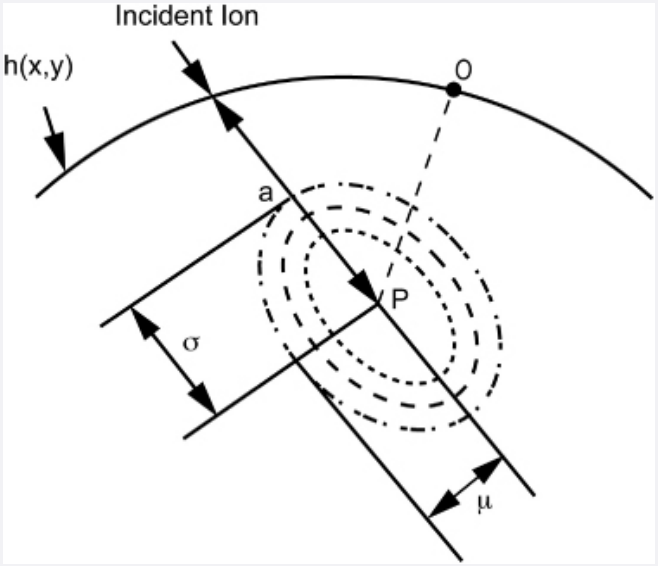

Headrick et al, J. Phys.: Condens. Matter, 2009, 21, 224005

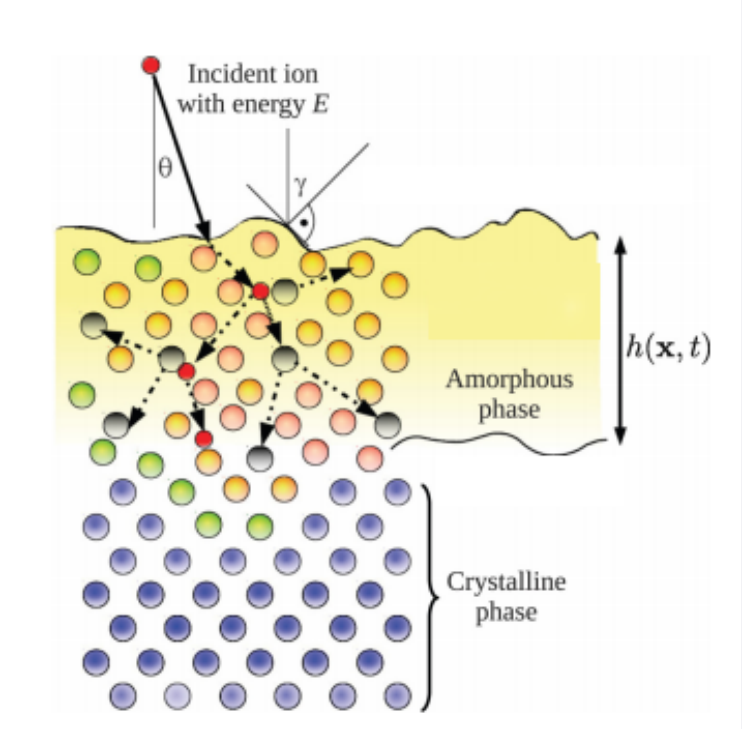

Adapted form Castro et al, PRB, 2012, 86, 214107

Sputtering

P. Sigmund (1969)

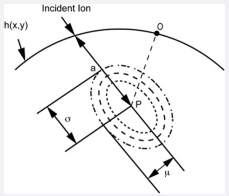

The sputtering yield Y (atoms/ion) is proportional to the energy deposited by the ion at the surface

J Yanagisawa et al., J Phys Condens Matter 2007 19 445002

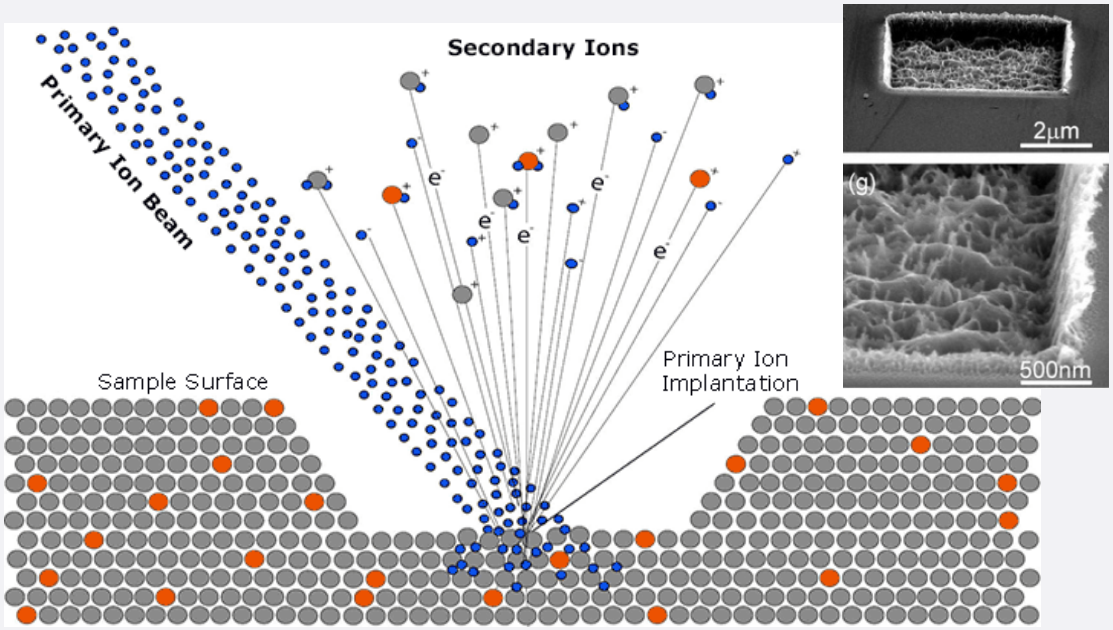

https://www.cameca.com

Angular dependence of the sputtering yield Y(θ) and of the deposited Energy E(θ):

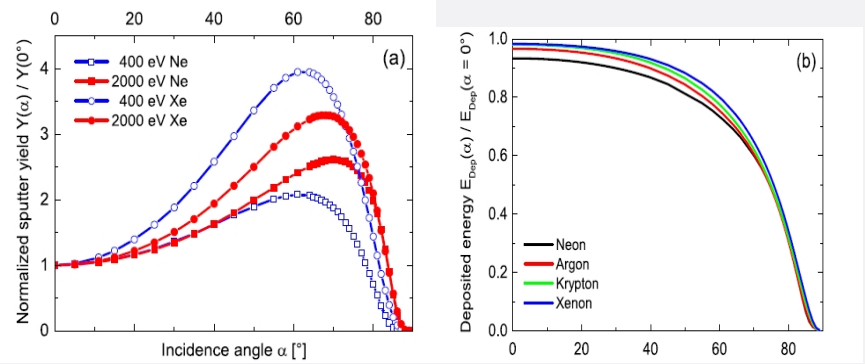

M. Teichmann et al., New Jour of Phys 2013 15 103029

Ion induced nanostructures: physical mechanisms

Credits: https://www.hzdr.de

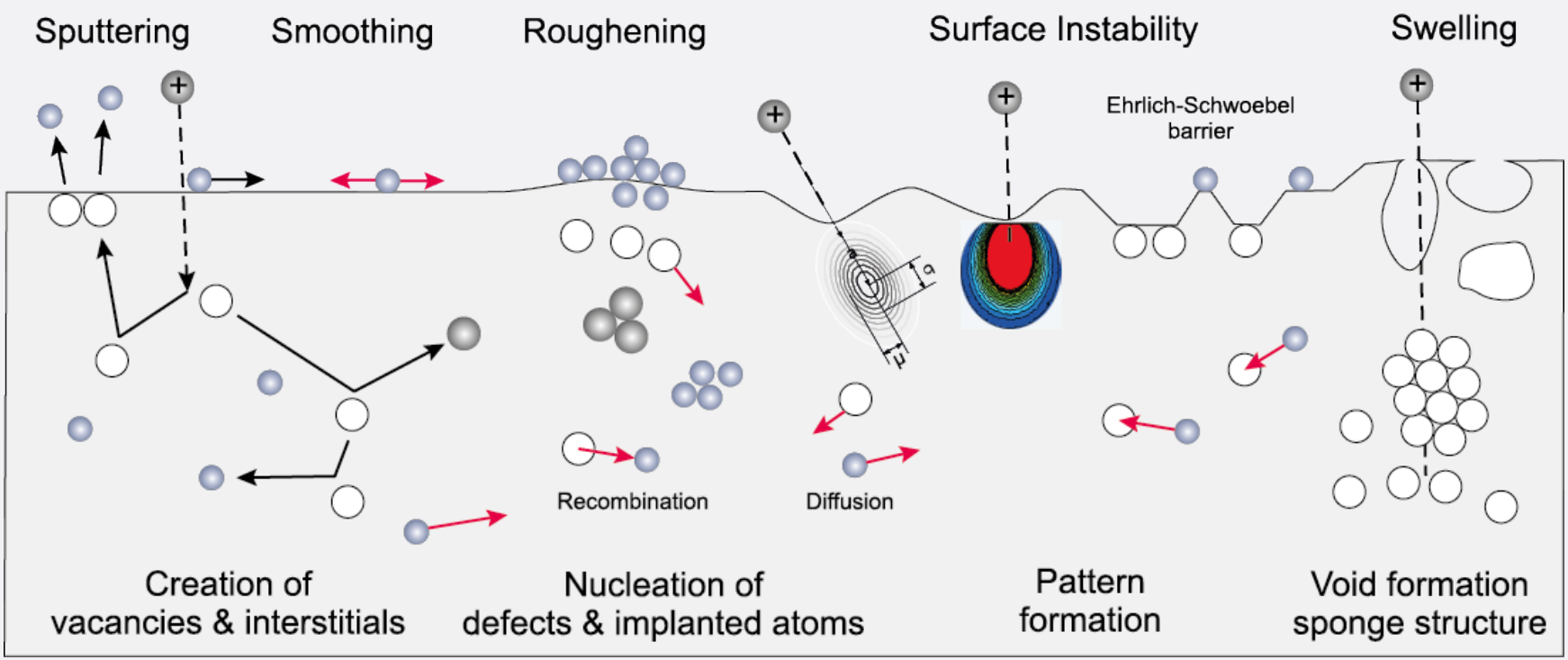

Ion induced nanostructures: physical mechanisms

W Chan et al., JAP 2007 101 121301

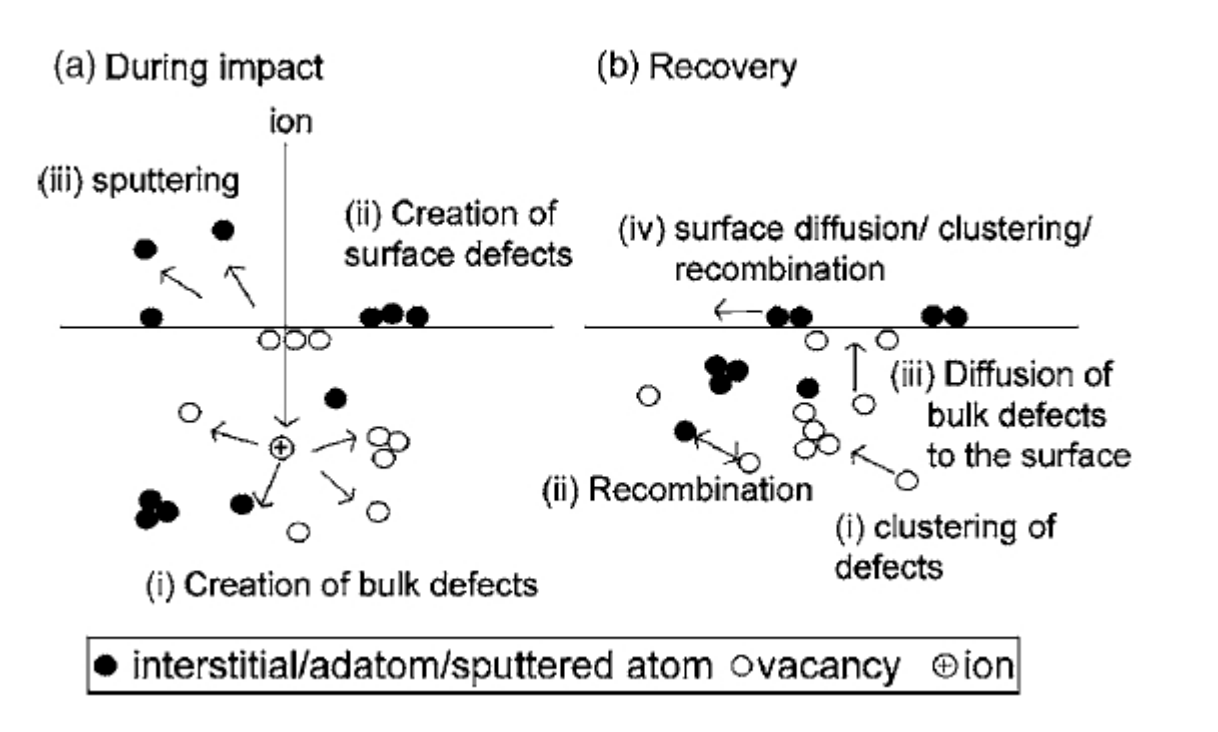

related to the ion damage

Cascades of atomic displacements by energetic ion impacts:

- Thin layer amorphized and stressed
- Crater→ surface redistribution effects
- Sputtered atoms

counteracting relaxations

- Thermal diffusion
- Ion-induced viscous flow
- Defect recombination
- Athermal diffusion

pattern production in a controlled & reproducible fashion

T, ϑ ,Φ, E…

Experimental parameters

Theories and Models

$$\frac{\partial h}{\partial t} = -v_0 + \frac{\partial v_0}{\partial \vartheta}\frac{\partial h}{\partial x} + A_x \frac{\partial^2 h}{\partial x^2} + A_y \frac{\partial^2 h}{\partial y^2} - B\nabla^4 h,$$

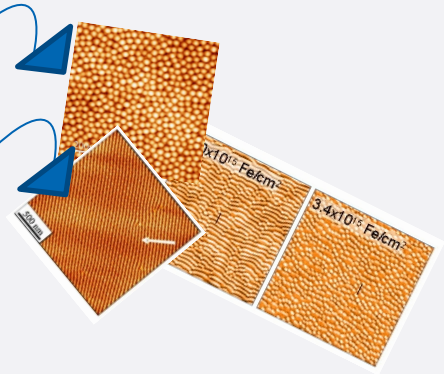

Nanopatterns

Understanding a subset of mechanisms for a subset of experimental parameters

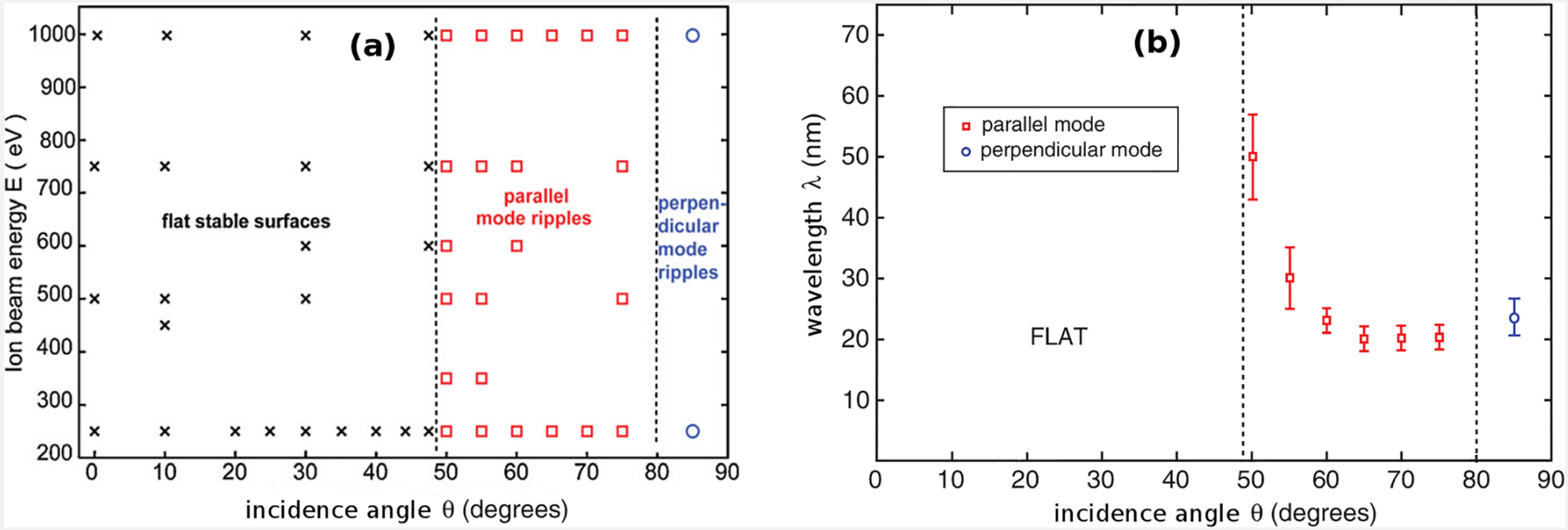

S. Norris et al., Appl. Phys. Rev. 2019 6 011311

Understanding a subset of mechanisms for a subset of experimental parameters

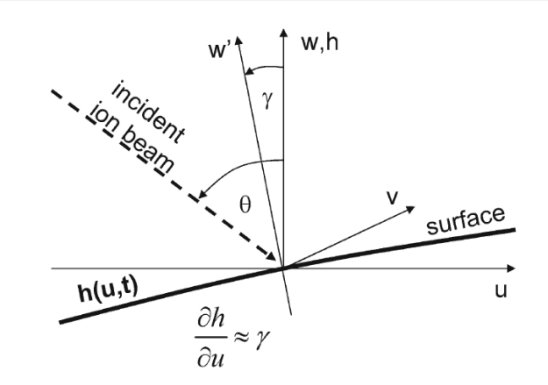

H. Hofsaess, Appl. Phys. A 2014 14 401

S. Macko et al., Nanotechnology 2010 21 085301

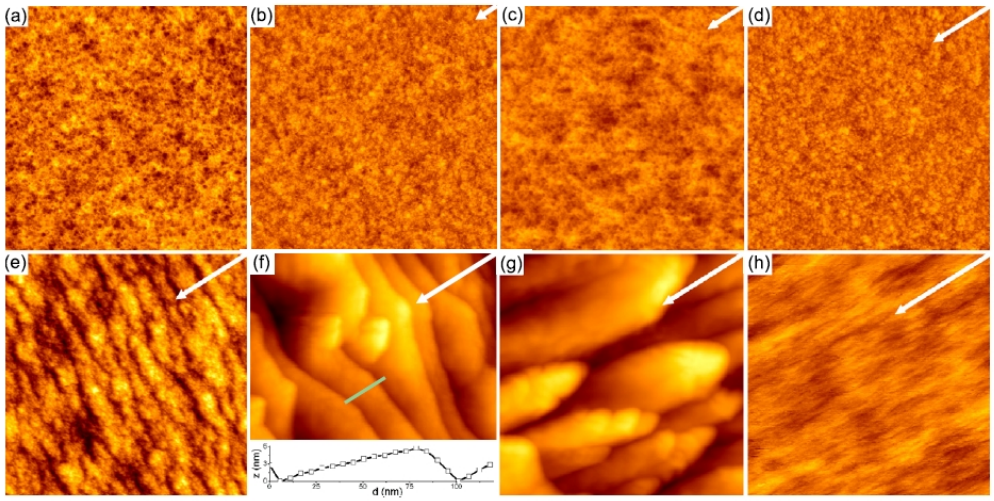

Figure 1. STM topographs of Si(100) after a fluence of $2 \approx 10^{22}$ ions m^{-2} 2 keV Kr^+ at 300 K. The angle of incidence ϑ with respect to the surface normal is (a) 0°, (b) 15°, (c) 26°, (d) 45°, (e) 60°, (f) 75°, (g) 79° and (h) 83°. The image size is for (a)–(d) and (h) 316 nm × 316 nm and in (e)–(g) 625 nm × 625 nm. The white arrows in (b)–(h) indicate the ion beam azimuth. The corrugation Δz is 3 nm in (a)–(e) and (h) and 30 nm in (f) and (g). Inset in (f): height profile along line indicated in (f).

Si surfaces irradiated by Kr^+ E= 2000 eV, $\Phi = 2 \times 10^{18}$ ions/cm^2

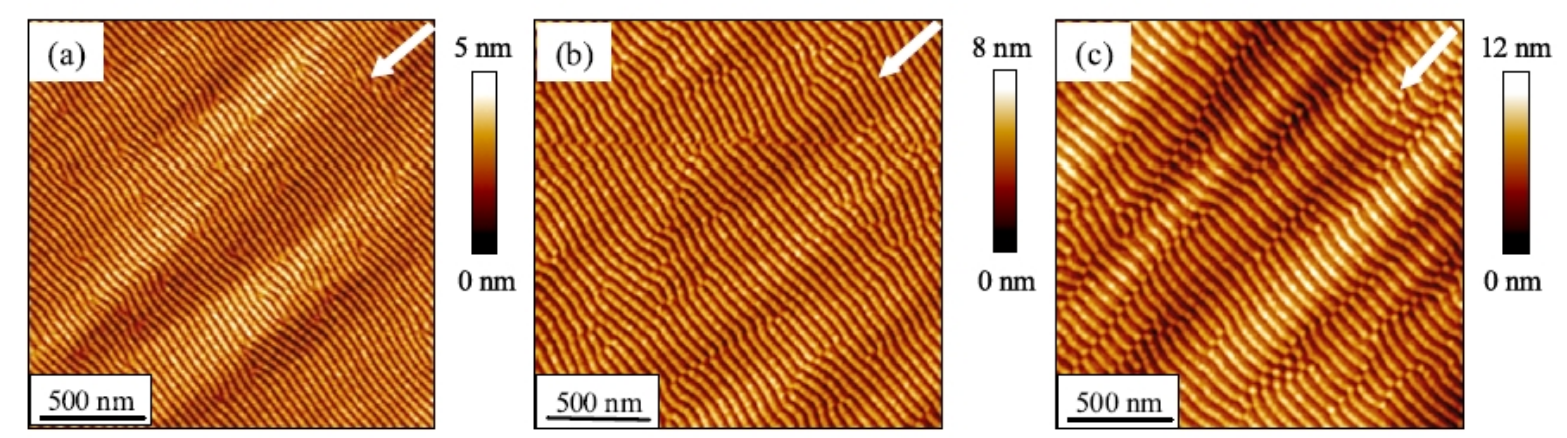

Si surfaces irradiated by Ar^+ at 15°, E=800 eV, 1200eV, 2000 eV, $\Phi = 6.7 \times 10^{18}\ cm^{-2}$

B. Ziberi et al., JPCM 2009 21 224003

Type I and Type II instabilities

$$h_1 = h_{11} \exp\left[R(\mathbf{q})t + i\mathbf{q}\cdot\left(\mathbf{x} + \frac{\psi(\mathbf{q})\mathbf{q}}{|\mathbf{q}|^2}t\right)\right]$$

S. Norris et al., Appl. Phys. Rev.2019, 6, 011311

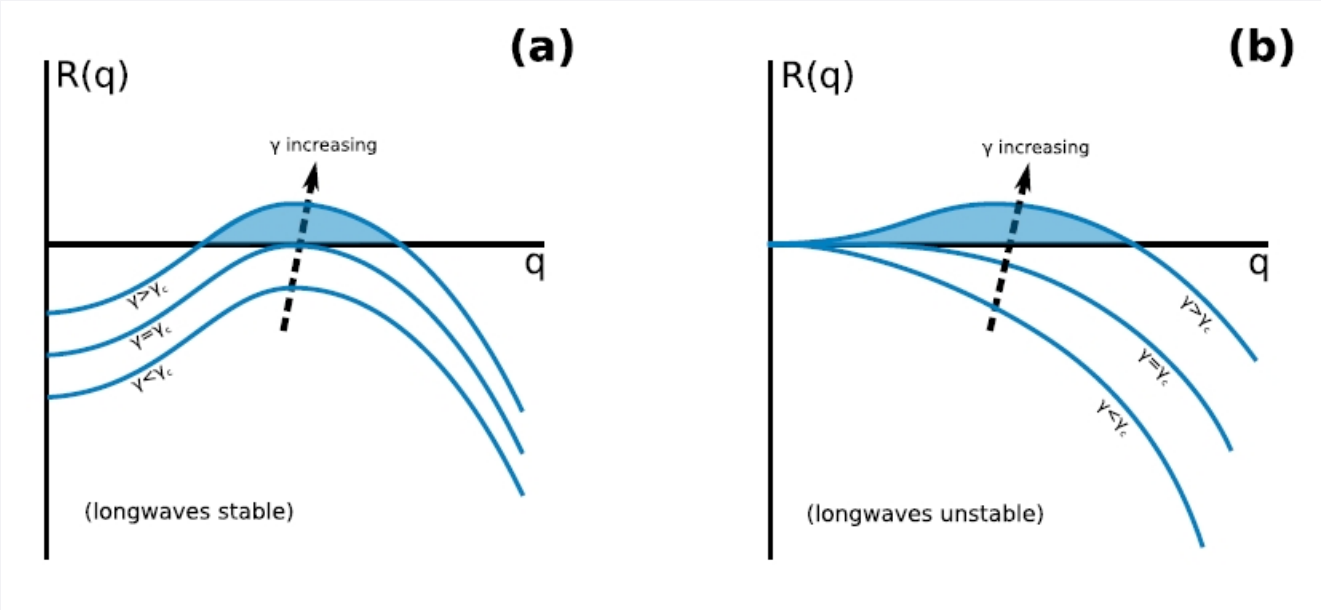

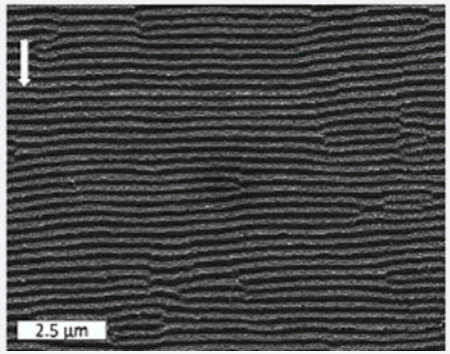

R. Dell'Anna et al,

RSC Advances 2017 7 9024

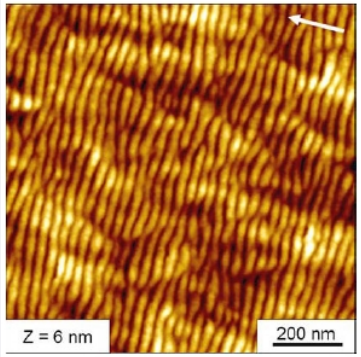

M. Teichmann et al.,
New Jour of Phys 2013 15 103029

Understanding a subset of mechanisms for a subset of experimental parameters

D. Datta et al, Appl Surf Sci 2016 360 131

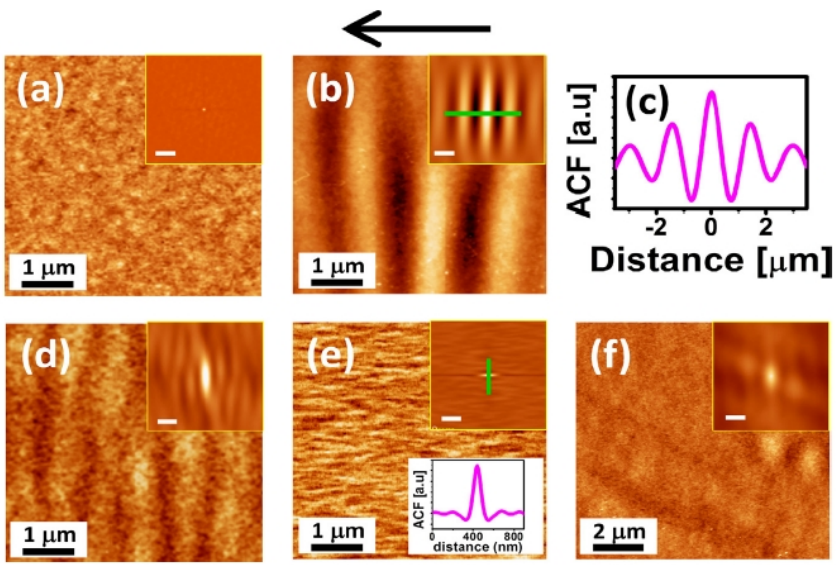

Ge surfaces irradiated by 100 keV Kr^{+} to the fluence of 3×10^{18}ions cm^{-2}

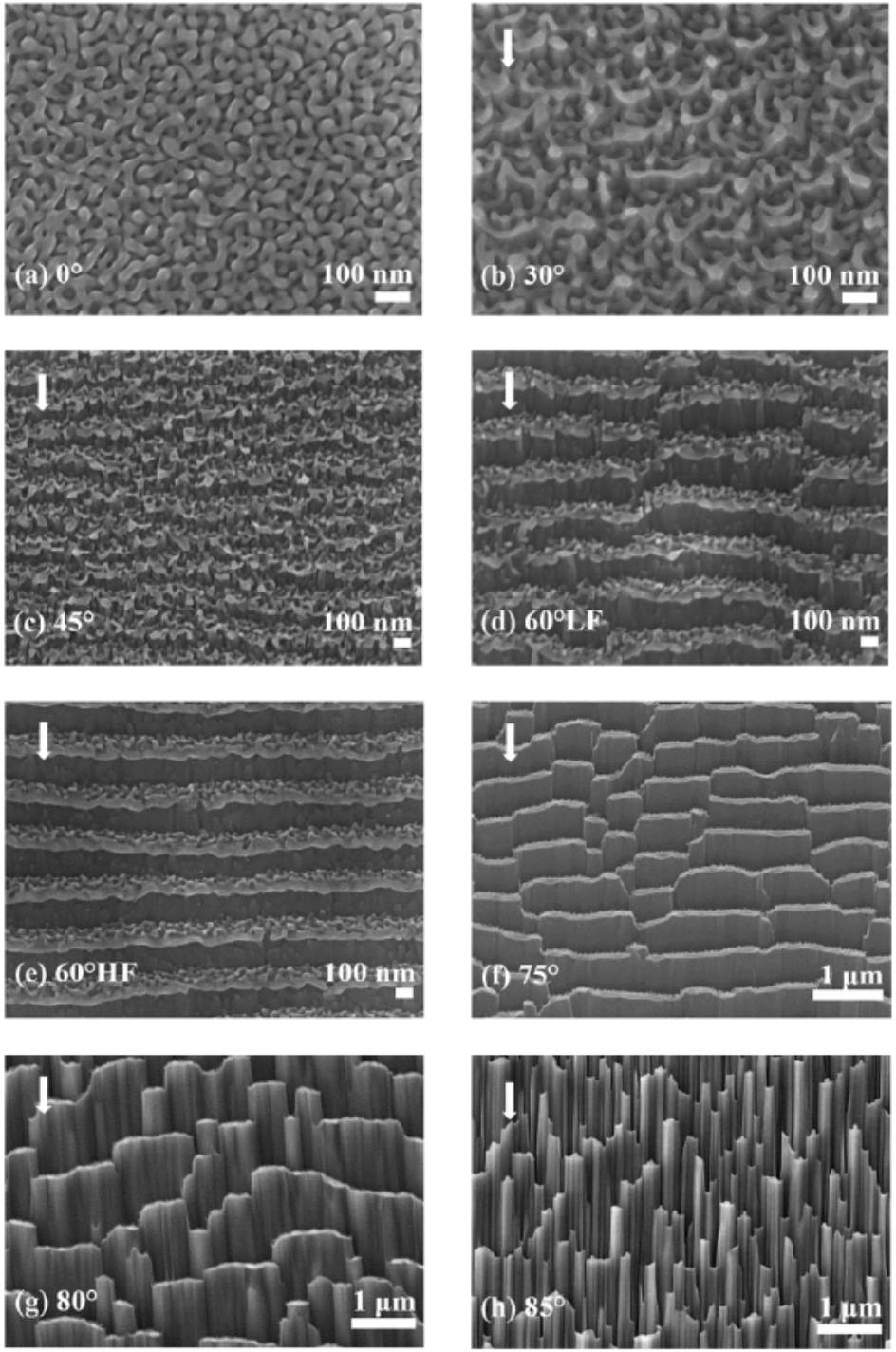

Ge surfaces irradiated by

Au+ E= 26 keV,

$\Phi = 5 \times 10^{16}$ ions cm^{-2}

R. Dell'Anna et al, JPCM 2018 30 324001

It-fab Italian Network for Micro and Nano Fabrication

continuum models

T. Som & D. Kanjilal Eds,
Nanofabrication by ion beam sputtering, 2013

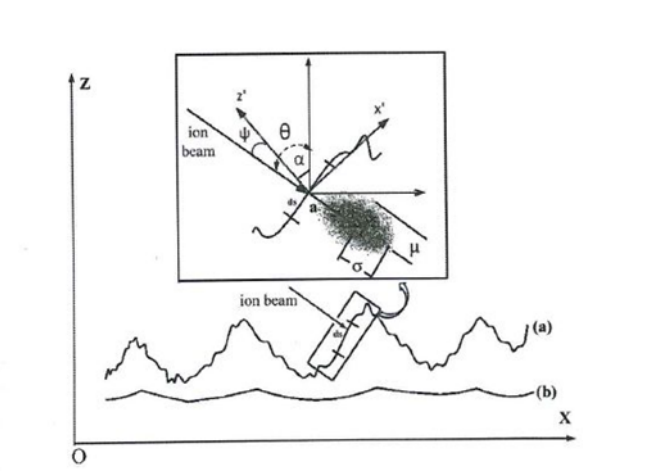

M A Makeev et al., Nucl. Instruments Methods Phys. Res. B 2002 197 185

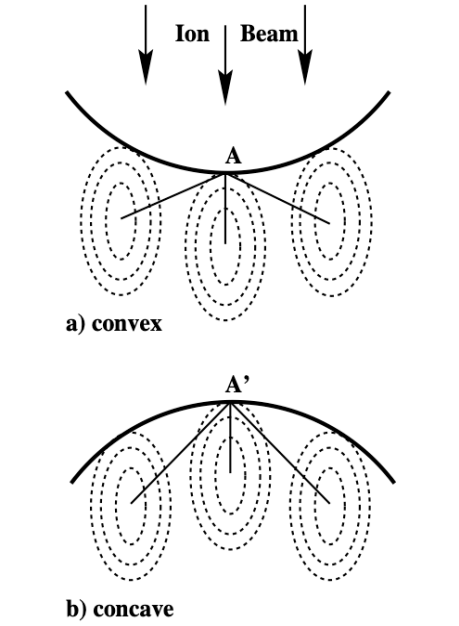

Linear continuum theory of Bradley & Harper for pattern formation

$$\frac{\partial h}{\partial t} = -v_0 + \frac{\partial v_0}{\partial \vartheta}\frac{\partial h}{\partial x} + A_x \frac{\partial^2 h}{\partial x^2} + A_y \frac{\partial^2 h}{\partial y^2} - B\nabla^4 h,$$

small slope approximation

competition between a roughening process by surface sputtering and smoothening process by surface diffusion

continuum models

Credits: https://www.hzdr.de

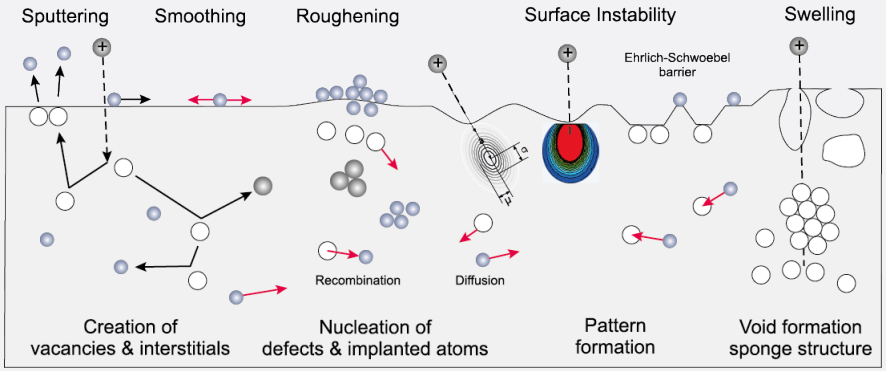

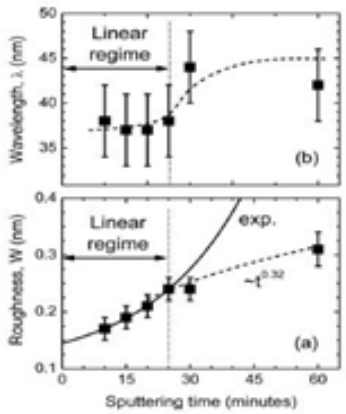

FIG. 5. Time evolution of the (a) surface roughness and (b) ripple wavelength for $E = 700$ eV, $J_0 = 30\ \mu\mathrm{A\,cm^{-2}}$ and $\theta = 55°$. The solid line in (a) is an exponential fit in the linear regime, while the dashed line is a power-law fit in the nonlinear regime with exponent 0.32. The dashed line in (b) is a guide to the eye. The time regime in which the wavelength grows with time (*coarsening*) starts at $t \simeq 25$ min, as indicated by the vertical dotted line; this is a signature of the onset of nonlinear effects. At shorter times the wavelength is almost constant. The same crossover time separates exponential from power-law behavior for the roughness.

M. Castro et al, PRB, 2012, 86, 214107

The (noisy) anisotropic Kuramoto-Sivashinsky equation

$$\frac{\partial h}{\partial t} = -v_0 + \frac{\partial v_0}{\partial \vartheta}\frac{\partial h}{\partial x} + A_x\frac{\partial^2 h}{\partial x^2} + A_y\frac{\partial^2 h}{\partial y^2} - B\nabla^4 h - B_{I,x}\frac{\partial^4 h}{\partial x^4} - B_{I,xy}\frac{\partial^4 h}{\partial x^2 \partial x^2} - B_{I,y}\frac{\partial^4 h}{\partial y^4}. + \frac{\lambda}{2}(\nabla h)^2 + \eta(x, y, t).$$

-ah

BH

Kinetic roughening

aeolian sand dunes

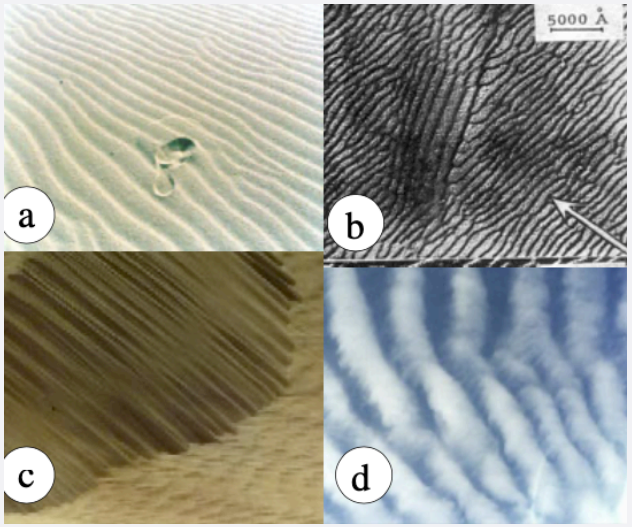

$$\partial_t h = \sum_{i=x,y} \left[-\nu_i \partial_i^2 h + \lambda_i^{(1)} (\partial_i h)^2 \right] + \sum_{i,j=x,y} \left[-K_{ij} \partial_i^2 \partial_j^2 h + \lambda_{ij}^{(2)} \partial_i^2 (\partial_j h)^2 \right].$$

The hydrodynamic model

Generalization of continuum theory: it retrieves all the features of the BH theory in the linear and nonlinear regimes;

T. Aste et al. New J Phys, 2005, 7, 122

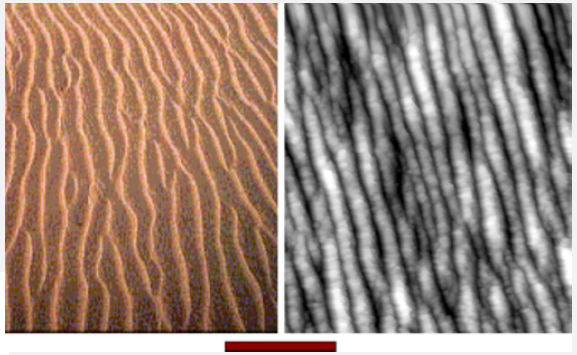

- Diversity of materials and similarities in morphologies → some kind of universality
- Dependence on irradiation parameters

It-fab Italian Network for Micro and Nano Fabrication

Nano-porous Ge and rippled Ge by ion irradiation

MNF-FBK, Trento

HZDR, Dresden

Ge surfaces irradiated with 26 keV Au ions at 5×10^{16} cm^{-2} fluence and varying angles

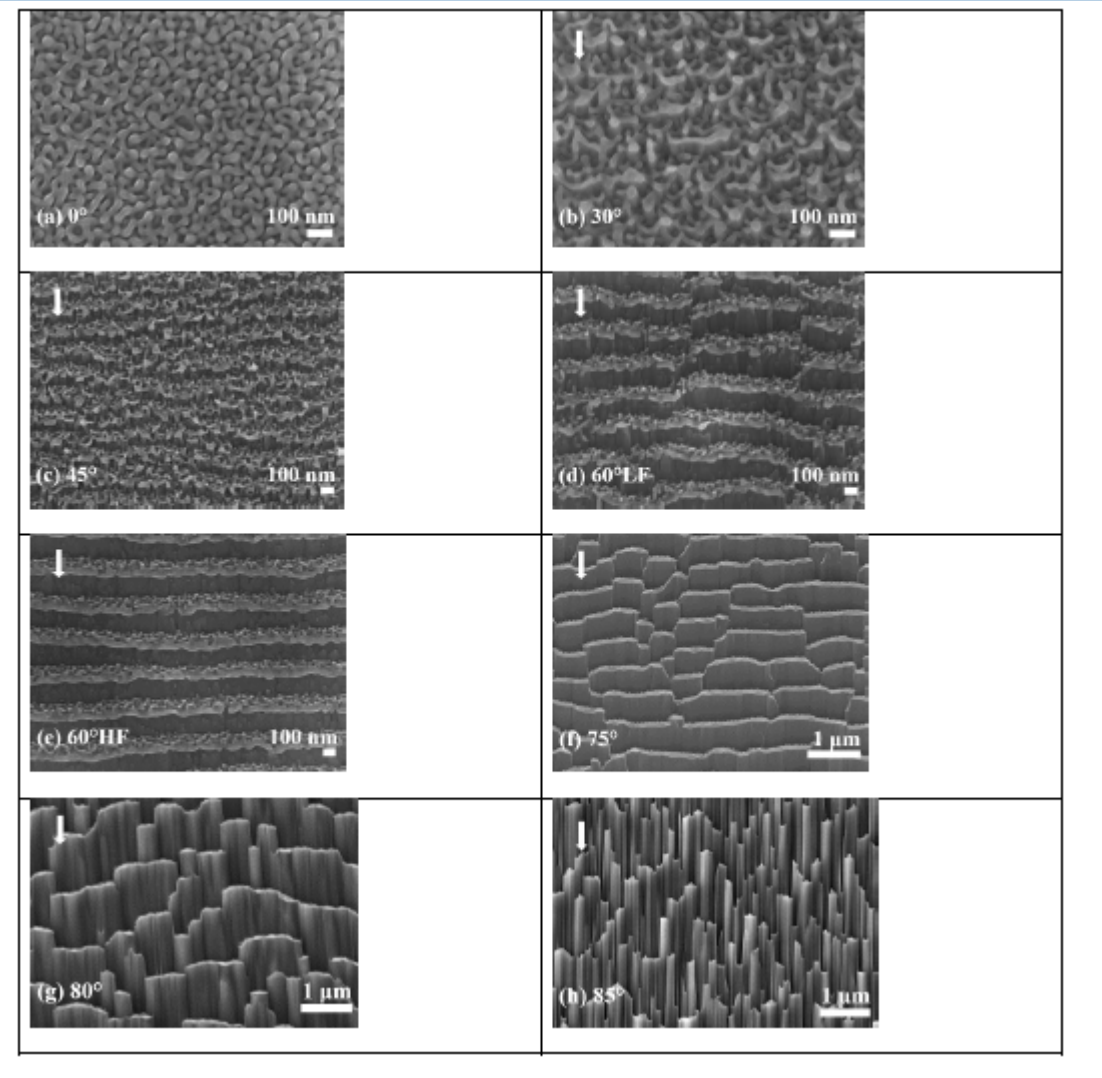

R. Dell'Anna et al, JPCM 2018 30 324001

Au low energy/ oblique incidence of Germanium

Au^+ 26 keV – 60° - vs. ion fluence

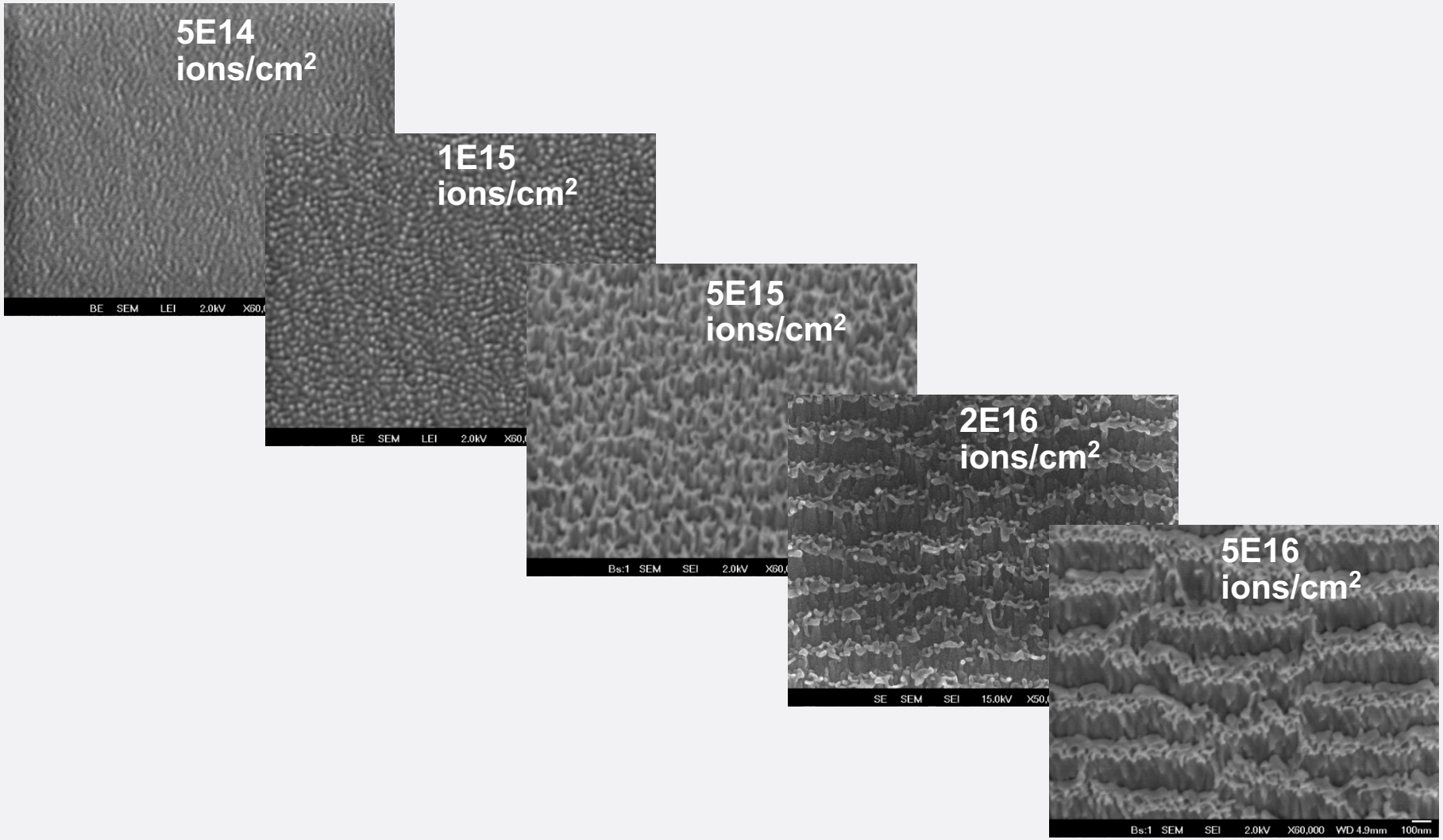

Nanoripples produced on Ge substrates by Au ion beam irradiation

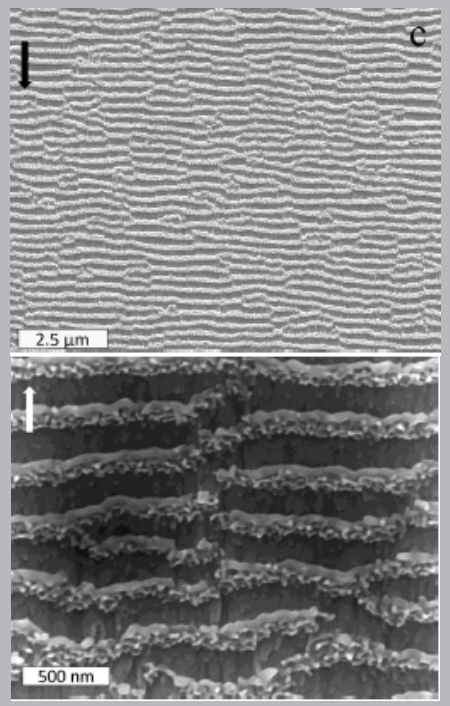

$\Psi = 1.0\times10^{17}$ ions·cm^{-2}

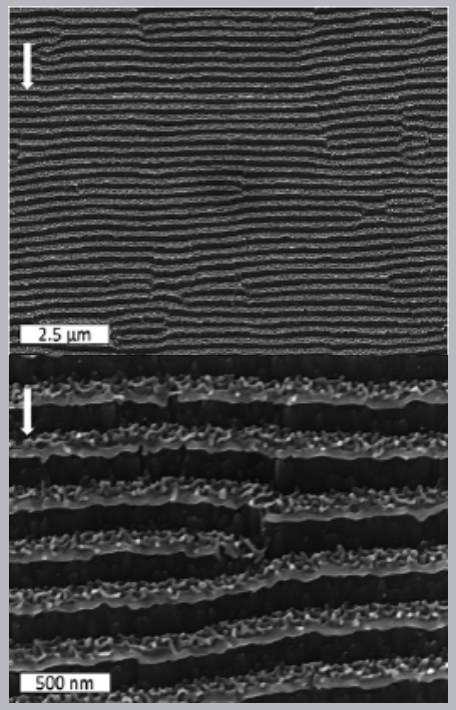

$\Psi = 4.3\times10^{17}$ ions·cm^{-2}

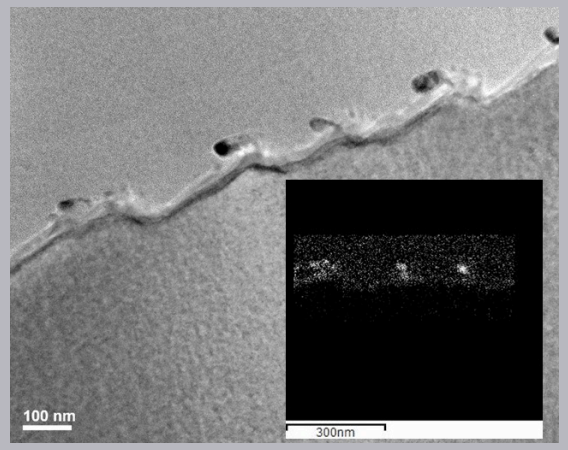

$\Psi = 5.0\times10^{16}$ ions·cm^{-2}

2D EDX map of Au Lb2 emission line, at 11.5847 keV

R. Dell'Anna et al, J. Phys.: Condens. Matter 30 324001 2018

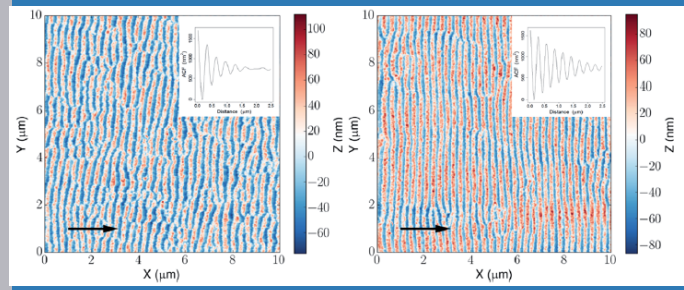

Au low energy/ oblique incidence of Germanium
Au^+ 5E16 cm^{-2}/ 26 keV – 60° - CROSS SECTIONS

SEM, tilted view

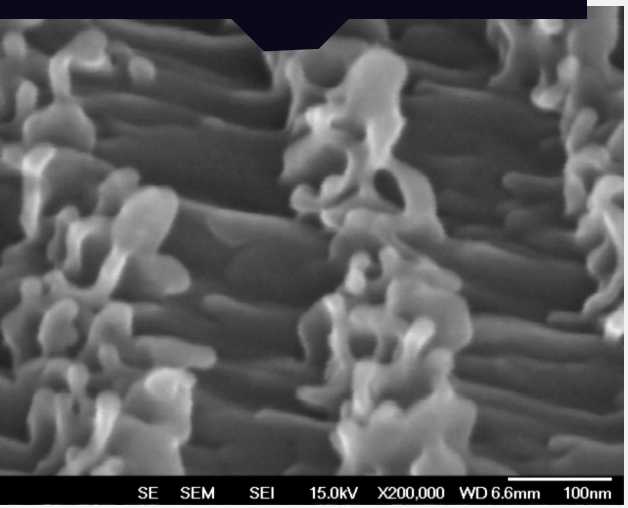

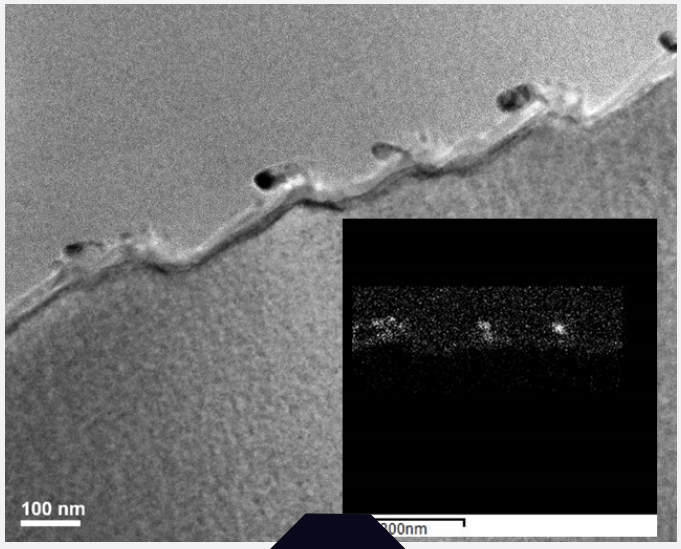

X-TEM

- Cross sections confirm the presence of nanowires on top of the ripple-crests.
- Nanowires are curled, in the opposite direction with respect to the ion beam.
- On top of the nanowires, there are particles very rich in Au (EDX image, Au L2b2 line, ~11600 eV, left).

X-TEM

An amorphous thick layer is present on the side of the ripple facing the beam, whereas it is much thinner on the other side.

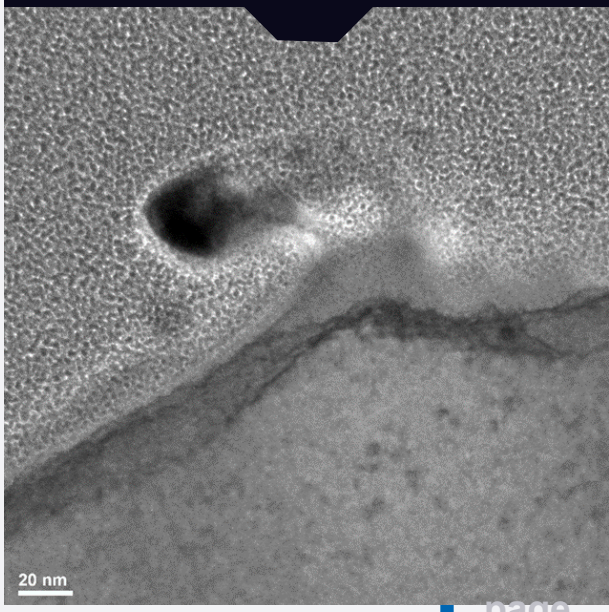

Hierarchical Ge nanoripples as templates for bioactive surfaces

MNF-FBK, Trento

NEST, Pisa

HZDR, Dresden

R. Dell'Anna, C. Masciullo et al., RSC Adv., 2017, 7, 9024

C. Masciullo, R. Dell'Anna et al., Nanoscale, 2017,9, 14861

the rationale behind

development of artificial neuronal interfaces for nerve-regeneration devices

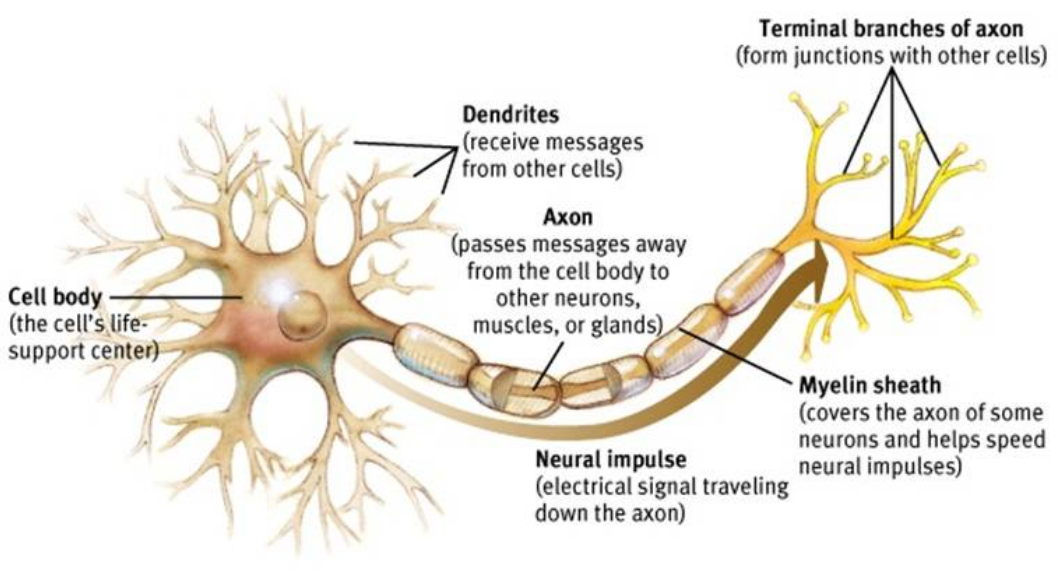

www.csun.edu/~cmm14283/PSY%20150/handouts/NeuronDiagram.doc

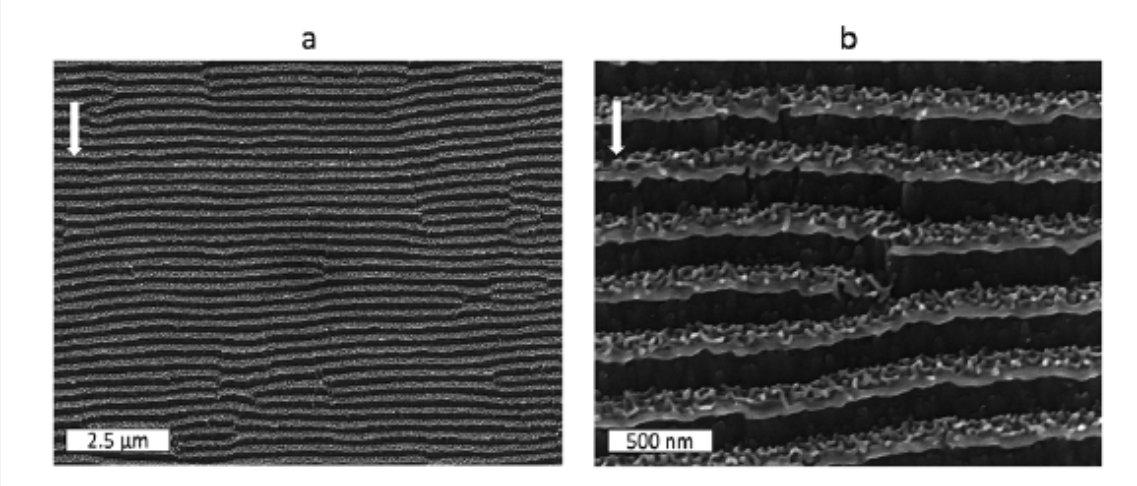

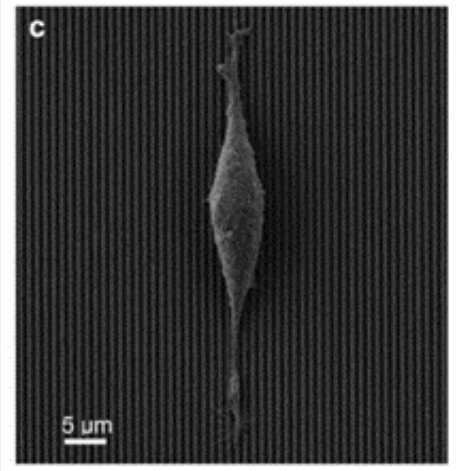

The substrate

Ge surface irradiated with 26 keV Au ions at 4.3×10^{17} cm^{-2} fluence and 60° incidence angle

the intermediate mold

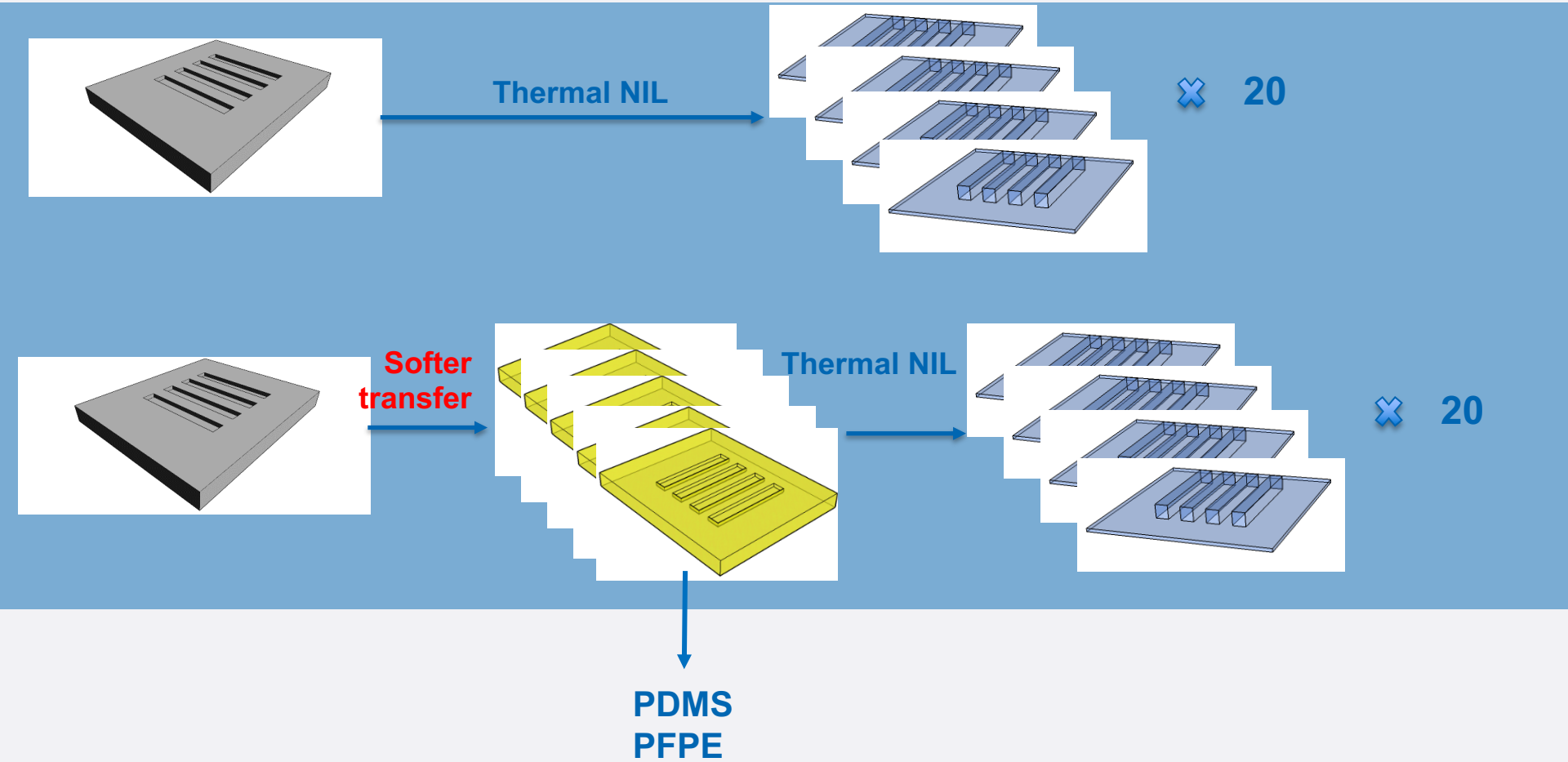

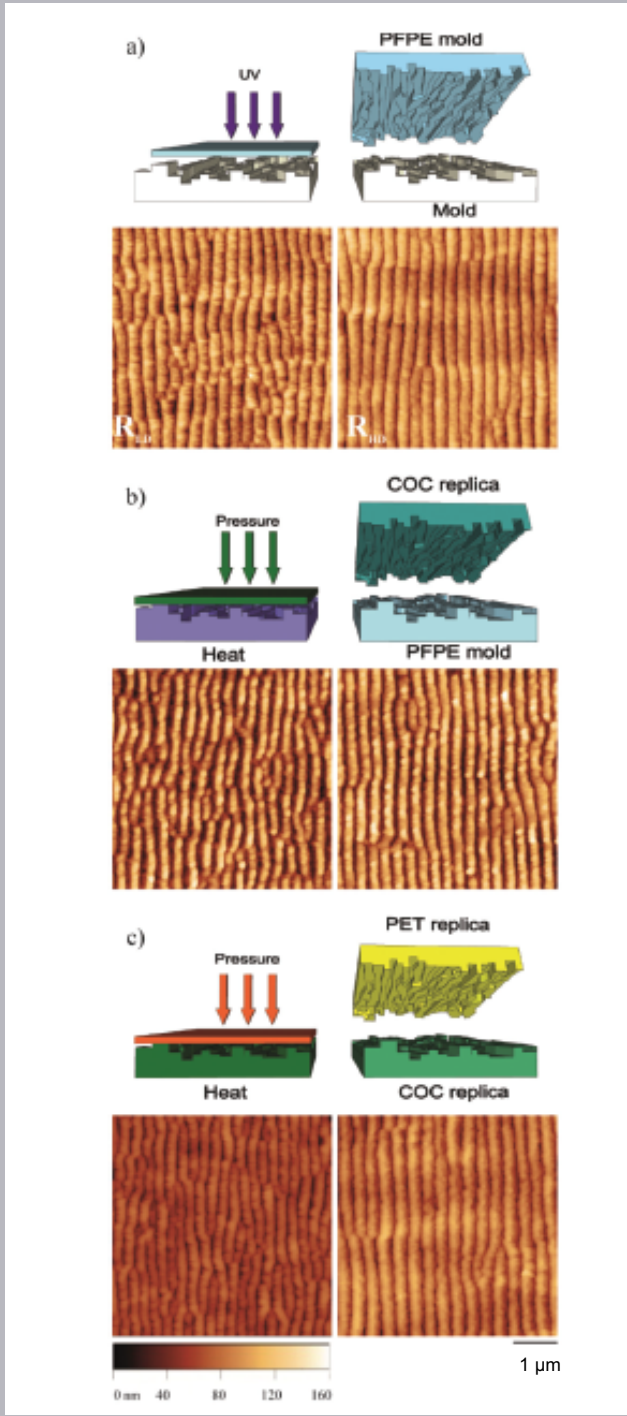

The 3-step embossing process

From Ge molds
to
polyethylene terephthalate
(PET) substrates

output

$\Psi = 4.3\times10^{17}$ ions·cm⁻

$\Psi = 1.0\times10^{17}$ ions·cm^{-2}

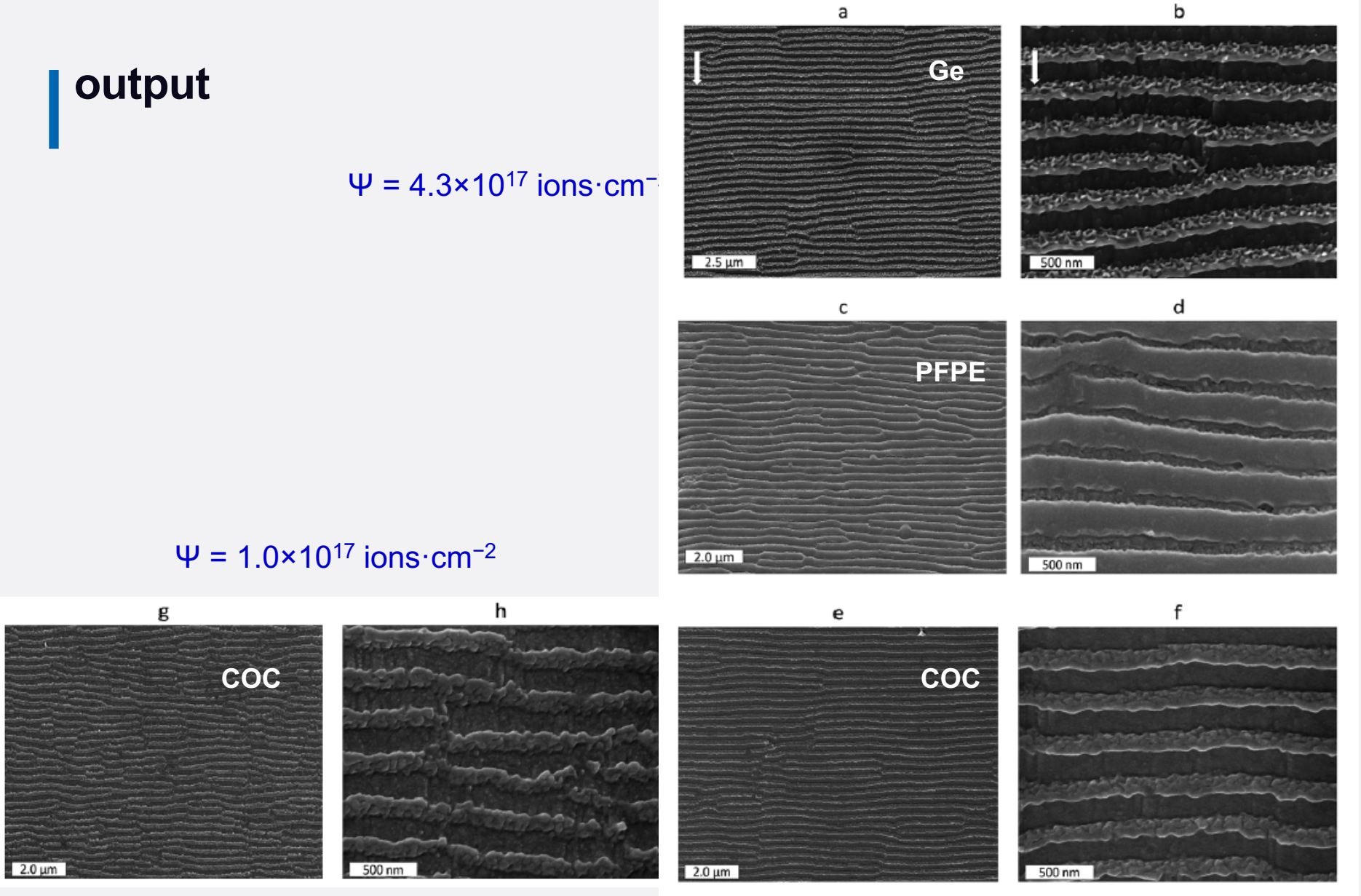

R. Dell'Anna, C.Masciullo et al, RSC Adv 7 9024 2017

the 3-step embossing process

Ge

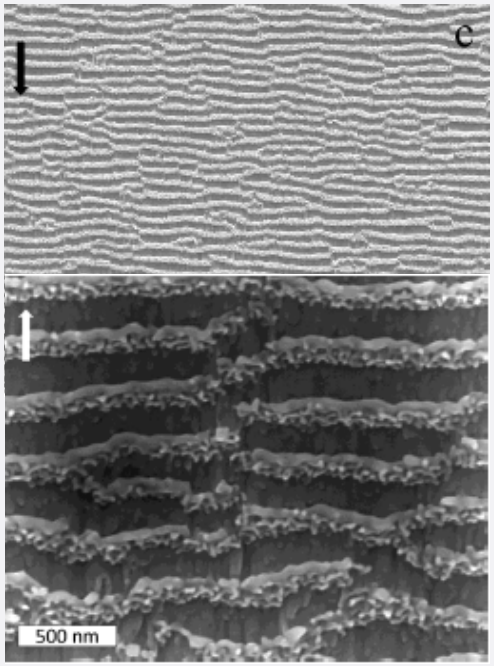

1.0×10^{17} ions·cm^{-2}

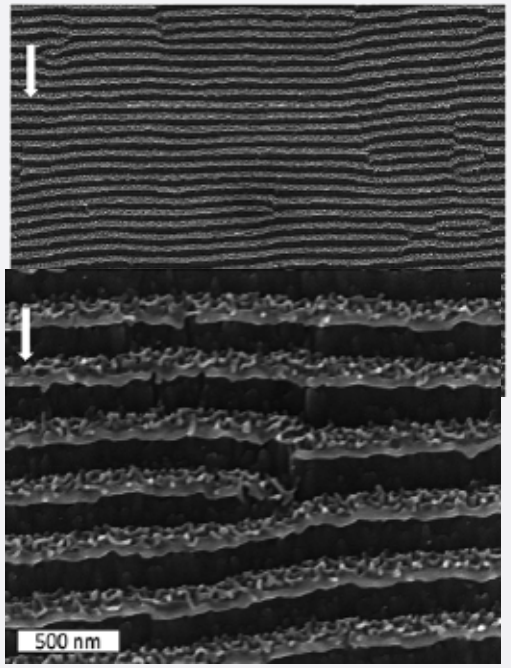

4.3×10^{17} ions·cm^{-2}

PET

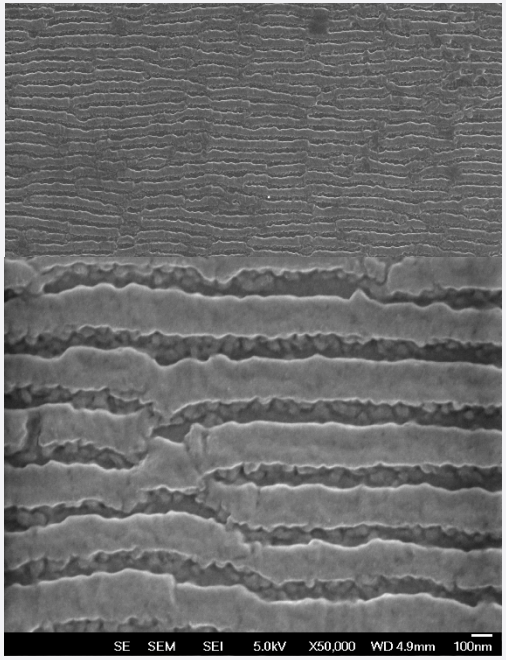

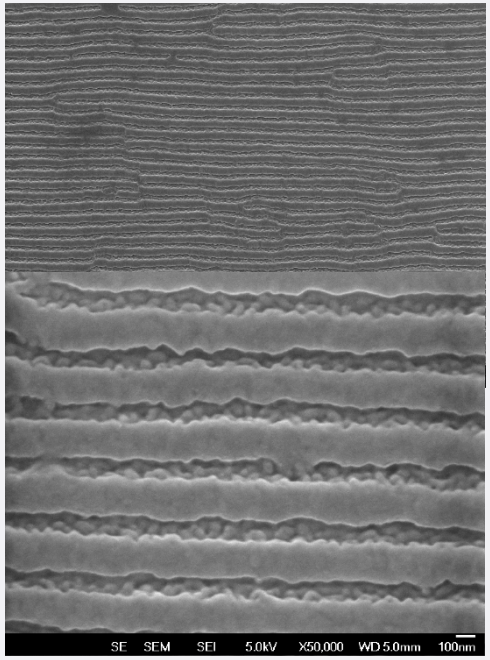

C Masciullo, R Dell'Anna et al, Nanoscale 9 14861 2017

It-fab Italian Network for Micro and Nano Fabrication

Cellular behavior

Schwann cells

1. adhesion and viability
2. spatial organization
3. filopodia orientation

1.

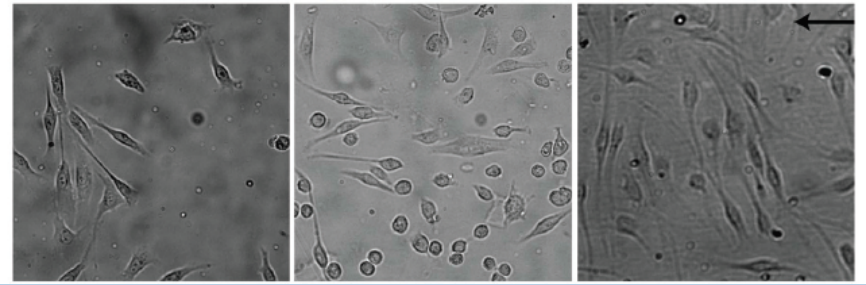

24 h

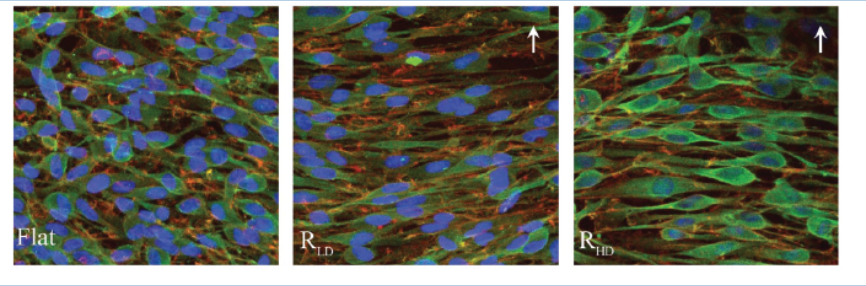

7 d

FLAT RIPPLE 1 RIPPLE 2

2.

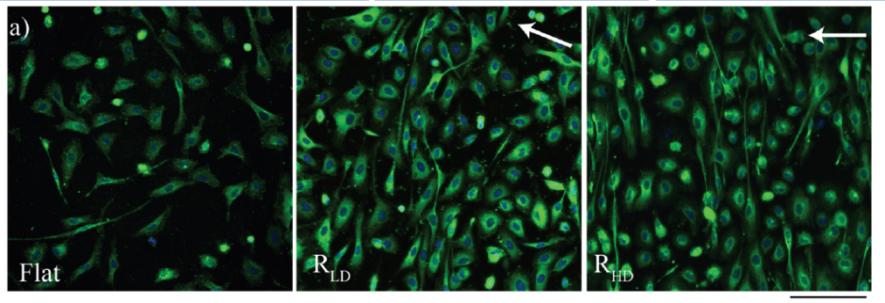

48 h

Cell angular distribution

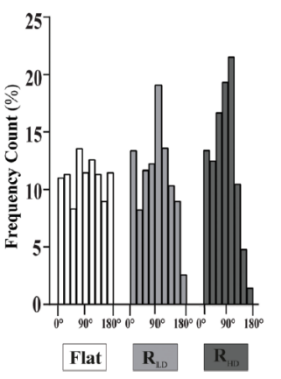

3.

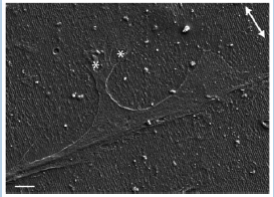

Filopodia

AFM and Raman study of graphene deposited on silicon surfaces nanostructured by ion beam irradiation

MNF-FBK, Trento

University of Sussex, Briighton

HZDR, Dresden

R. Dell'Anna, et al., J. Microsc., 2020

Bare Si samples	After graphene deposition	Implanted ion species	Energy (keV)	Fluence 10^{18} (ions/cm^{-2})	Incidence angle (°)
S1	G1	O+	1	1.0	50
S2	G2	O+	1	2.0	55
S3	G3	O+	1	2.0	50

1.

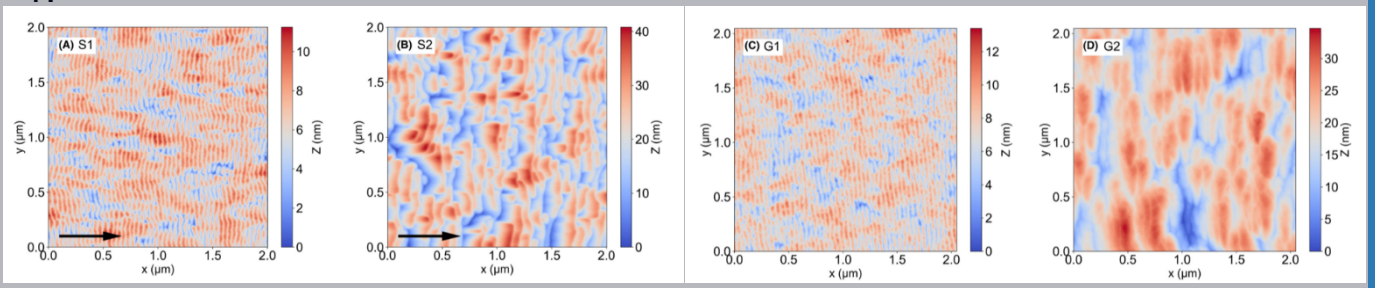

2.

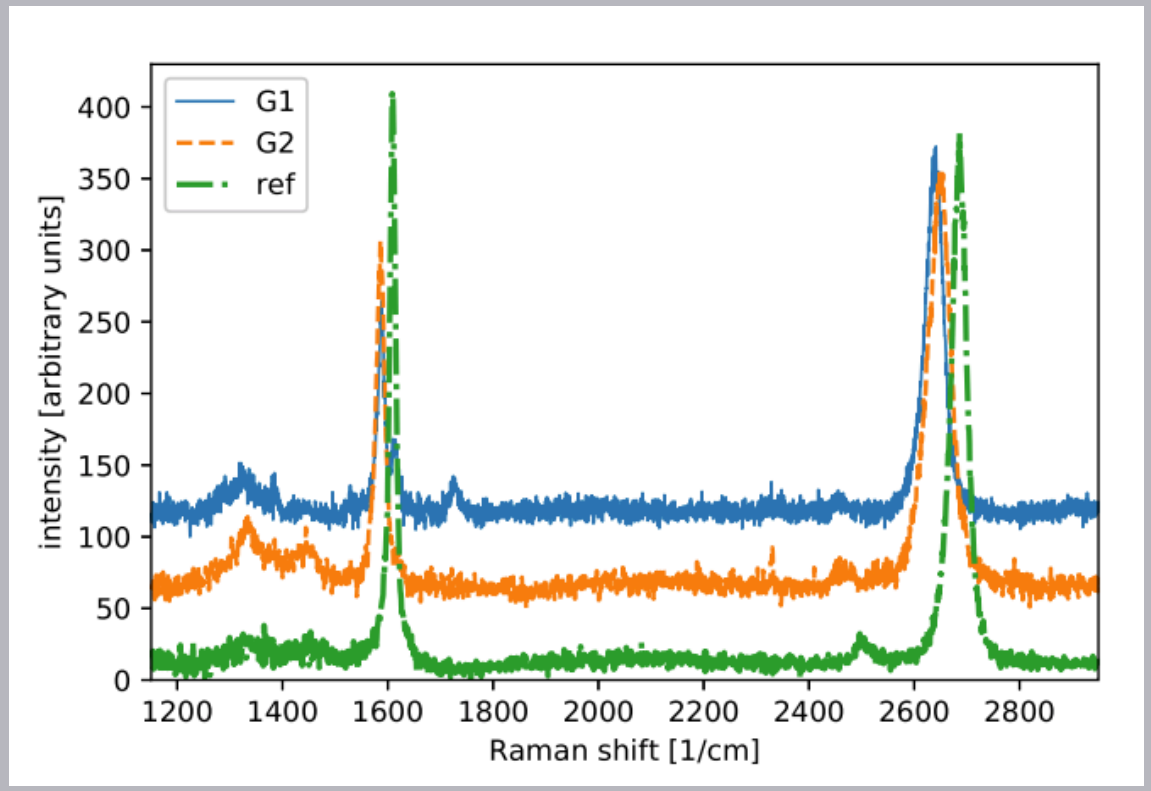

Raman from graphene deposited on Si nanostructured surfaces

1. AFM topography of the O+ irradiated Si surface and subsequent graphene deposition;

2. Raman spectra from graphene covered samples G1 and G2 and from CVD-grown graphene deposited onto a flat Si surface (reference)

uniaxial strain in the more conformal graphene sheet

R, Dell'Anna et al JMI 2020

Helmholtz-Zentrum Dresden-Rossendorf,
Institute of Ion Beam Physics and
Materials Research,

Fondazione Bruno Kessler,
Micro Nano Facility, Trento

thank you

NEST, Scuola Normale Superiore,
Istituto Nanoscienze-CNR, Pisa

UNIVERSITY OF SUSSEX
Department of Physics and Astronomy